

Joining of Dual-Phase Coated Steel Sheets DP600

Denis Cmorej, Ľuboš Kaščák

Department of Technology, Materials and Computer Support of Production,
Technical University of Košice, Košice, Slovakia, Europe

ABSTRACT

Currently, high-strength steels are increasingly used in the production of car bodies. Car manufacturers choose steel with good formability, fatigue resistance, and the ability to absorb impact energy. DP (dual-phase) steels verify the specific criteria mentioned above. Resistance spot welding is one of the most common methods of joining high-strength dual-phase steels. The paper focuses on the comparison of the properties of joints made by resistance spot welding. Selected properties were investigated by tensile test and metallographic observations. HCT600X + Z and HCT600X + ZF steel sheets were used for the experiments.

KEYWORDS: resistance spot welding, tensile test, metallography, HCT600X+Z, HCT600X+ZF

How to cite this paper: Denis Cmorej | Ľuboš Kaščák "Joining of Dual-Phase Coated Steel Sheets DP600" Published in International Journal of Trend in Scientific Research and Development (ijtsrd), ISSN: 2456-6470, Volume-5 | Issue-6, October 2021, pp.1102-1106, URL: www.ijtsrd.com/papers/ijtsrd47547.pdf



Copyright © 2021 by author (s) and International Journal of Trend in Scientific Research and Development Journal. This is an Open Access article distributed under the terms of the Creative Commons Attribution License (CC BY 4.0) (<http://creativecommons.org/licenses/by/4.0>)



I. INTRODUCTION

The most important aspects that are emphasized in the automotive industry include design, low vehicle weight, good formability, and the ability to absorb impact energy within specific body parts[1-2]. These aspects ensured the application of high-strength steel sheets for specific body parts [3].

One of the best known and most used high-strength steels is dual-phase (DP) steel, precisely because of the suitable properties. The dual-phase steels offer a combination of high strength and good formability because of their microstructure. Dual-phase steels are suitable to produce structural and safety parts in the automotive industry [4-6].

Resistance spot welding is one of the best known and most widely used methods of joining high-strength dual-phase steels. Resistance spot welding is a technology that creates joints without additional material with the assistance of a high-intensity welding current under the simultaneous action of the contact force created by the electrodes. One of the advantages of the technology is the high intensity of the process, as well as the ability to automate the

process. The load-bearing capacity of the joints as well as the resulting quality of the joints depends on the welding parameters and the type of material used. Spot resistance welding parameters include welding time, welding current, and electrode contact force[7-9].

The paper deals with the evaluation of the load-bearing capacity of joints as well as the metallographic observation of joints created by resistance spot welding. HCT600X + Z and HCT600X + ZF steel sheets were used in the experiments.

Methodology of experiments

One type of material was used for the experiment. The thickness of the tested steel sheets was 1.5 mm. The HCT600X + Z sheet was galvanized on both sides. The HCT600X + ZF sheet is known for zinc-iron(ZF) alloy coating, which provides better corrosion protection compared to only zinc coating.

Table I. shows the basic mechanical properties of the used materials. The chemical composition of steel sheets is shown in Table II.

Table I basic mechanical properties of the used materials

Material	Thickness [mm]	Rp _{0.2} [MPa]	Rm [MPa]	A ₈₀ [%]
HCT600X+Z	1.5	373	606	24.8
HCT600X+ZF	1.5	369	633	22.5

Table II Chemical composition of joined materials in wt [%]

Material	Chemical composition				
	C	Mn	Si	P	Al
HCT600X+ZF	0.080	1.78	0.01	0.014	0.045
	Nb	Ti	V	Mo	Cr
	0.002	0.001	0.002	0.179	0.211
HCT600X+Z	C	Mn	Si	P	Al
	0.09	1.89	0.26	0.014	0.026
	Nb	Ti	V	Mo	Cr
	0.001	0.003	0.002	0.002	0.21

Samples with dimensions of 90x40 mm with an interleaving length of 30 mm were used to creating joints by resistance spot welding. Dimensions of the samples were defined by the standard of STN 05 1122. Figure 1 shows the dimensions of a tested sample.

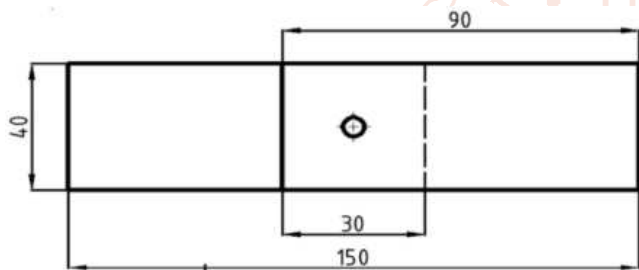


Fig 1 Dimensions of a tested sample

Resistance spot welding

For welding, a spot-welding machine BPK 20 was used. The CuCr electrodes (A2/1) according to the ON 42 3039.71 with a diameter of working area $d_e = 5$ mm were used in experiments.

For each type of sheet, 4 groups were created: A, B, C, D. Each group contains 5 samples. The samples were grouped according to the welding current I_4 is defined as the welding current. Tables 3 and 4 below show the welding parameters used for HCT600X+Z and HCT600X+ZF.

Table III welding parameters used for the HCT600X+Z material

HCT600X+Z	Welding parameters		
	Force Fz [kN]	Welding Current I_4 [kA]	Time Tw [per.] (1 per. = 0.02 s)
A	9.0	6	15 (300 ms)
B	9.0	6.5	15 (300 ms)
C	9.0	7	15 (300 ms)
D	9.0	7.5	15 (300 ms)

Welding parameters used for the HCT600X+ZF material

HCT600X+ZF	Welding parameters		
	Force Fz [kN]	Welding Current I_4 [kA]	Time Tw [per.] (1 per. = 0.02 s)
A	9.0	5	15 (300 ms)
B	9.0	5.5	15 (300 ms)
C	9.0	6	15 (300 ms)
D	9.0	6.5	15 (300 ms)

Tensile test

In the experiment, the load-bearing capacity of resistance spot welded joints and clinched joints were measured. The test was carried out on TIRA test 2300 (see figure 2).

The tensile test was carried out by STN 05 1122.

During the gradual loading of test specimens formed by spot resistance welding, their partial elongation to failure occurred. Subsequently, the maximum force F_{max} at which the failure occurred was deducted. The resulting measured values from the tensile test were subsequently recorded.



Fig 2 TIRA test 2300

Metallographic observation

The change in the microstructure of the materials HCT600X + Z and HCT600X + ZF, which occurred during the formation of joints by resistance spot welding, was analyzed by metallographic observation. A microscopic analysis of metallographic cross-sections was performed by using a KEYENCE VHX- 5000 light optical microscope (see Figure 3).

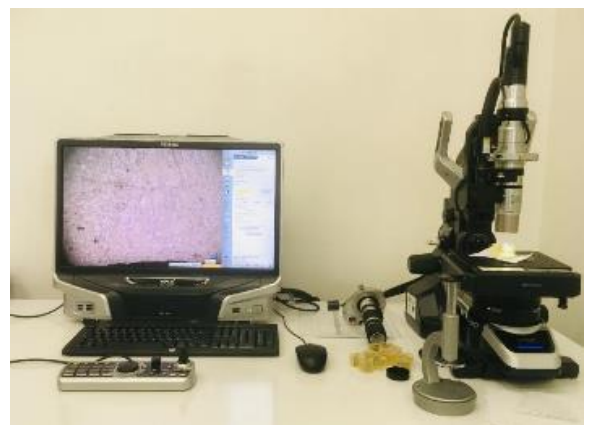


Fig 3 KEYENCE VHX - 5000

Result and discussion

Tensile test

The results of the tensile test are shown and described in the given section. Figure 4 shows load-displacement curves for the HCT600X + Z material. Figure 5 shows a graph of the average values of the load-bearing capacity for the HCT600X + Z material.

Figure 6 shows load-displacement curves for the HCT600X + Z material. Figure 7 shows a graph of the average values of the load-bearing capacity for the HCT600X + Z material.

The lowest value of load-bearing capacity of joints was measured on samples with the highest values of welding current (sample A): about 14 kN on the samples with HCT600X+Z, about 12 kN on the samples with HCT600X+ZF.

The highest value of load-bearing capacity of joints was measured on samples with the highest values of welding current (sample D): about 19.5 kN on the samples with HCT600X+Z, about 17 kN on the samples with HCT600X+ZF.

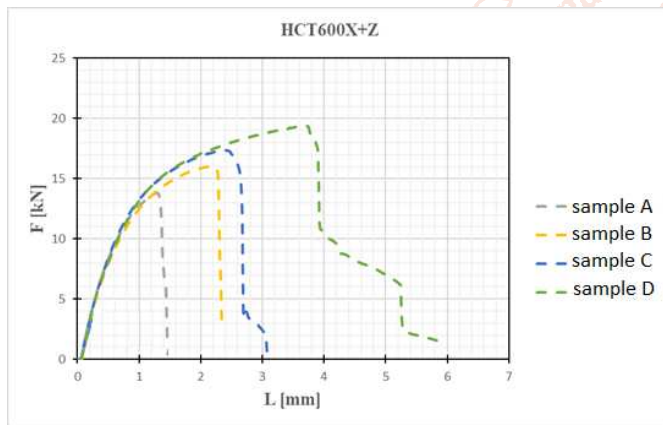


Fig 4 Load-displacement curves for the HCT600X+Z material

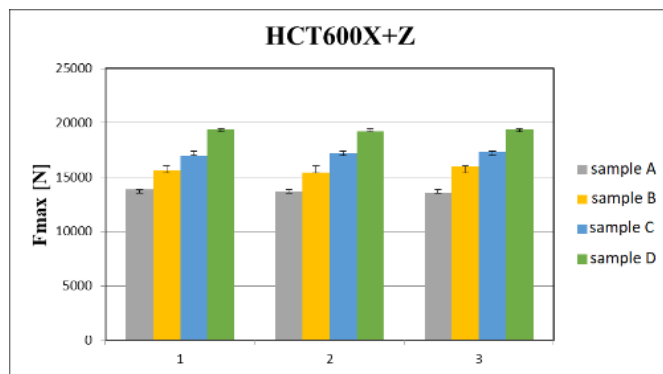


Fig 5 Graph of average values of the load-bearing capacity of joints after the tensile test for the HCT600X+Z material

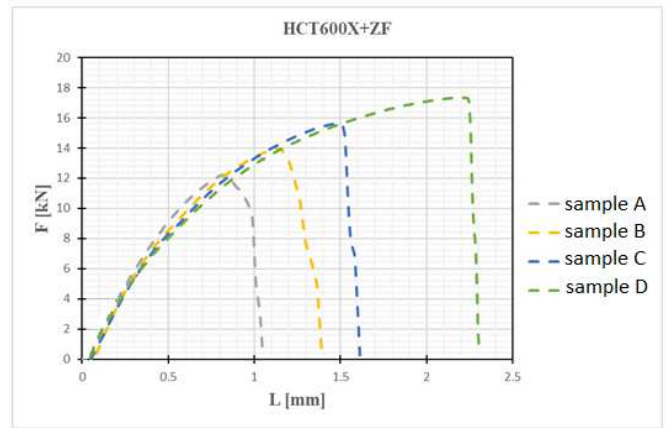


Fig 6 Load-displacement curves for the HCT600X+ZF material

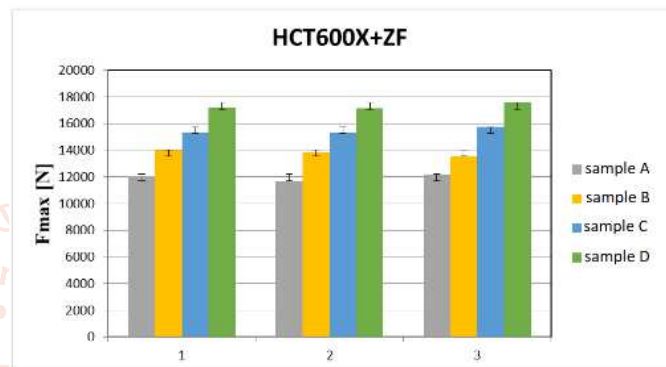


Fig 7 Graph of average values of the load-bearing capacity of joints after the tensile test for the HCT600X+ZF material

Metallographic observation

Metallographic observation of the joints was performed on the observed materials- HCT600X+Z and HCT600X+ZF. Metallographic observation was used in the assessment of the type of joint formed - cold or fusion joint. Microscopic observation was used to assess the occurrence of cracks and pores, whether it is a cold or fusion joint. The quality of welded joints can be assessed by means of a macrostructure on metallographic sections.

A comparison of the shape of the welded joint for the material HCT600X + Z can be seen in figure 8. From metallographic observations, it can be determined that a dendritic structure was formed in the core of the weld nugget. It can also be deduced that during the joining of the materials, a fusion weld was formed with the characteristic areas of the base material, the heat-affected zone, and the weld nugget. With increasing values of the welding current, hot cracks also occurred in the heat-affected zone.

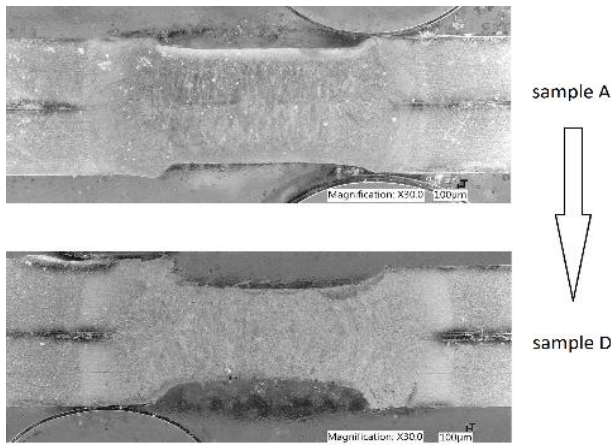


Fig 8 Microstructure of a sample made of HCT600X+Z

In Figure 9, a transition from the heat-affected zone to the base material can be observed. At low welding currents, the transition is smoother. With increasing values of the welding current, the transition from the heat-affected zone to the base material is more specific.

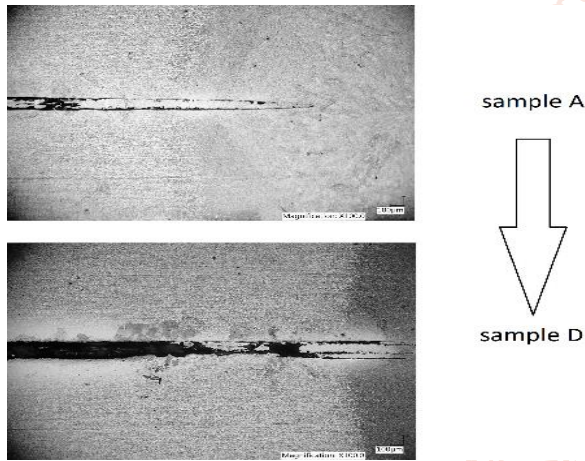


Fig 9 Microstructure of a sample made of HCT600X+Z – position base material – heat-affected zone

Figure 10 shows the structure of the core in a welded joint. With SAMPLE - D, a significant porosity can be observed in the weld metal structure, which is caused by the high welding current.

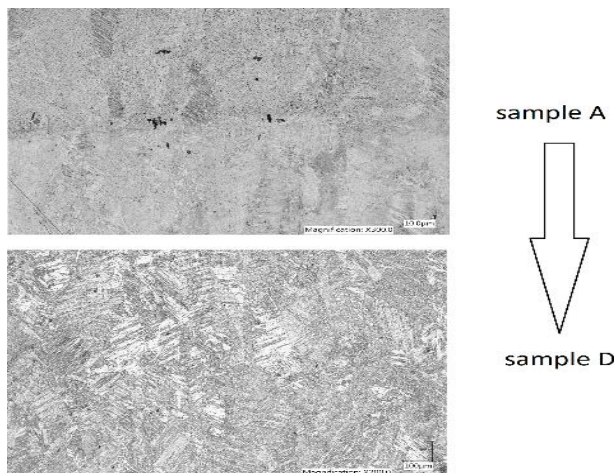


Fig 10 Microstructure of a sample made of HCT600X+Z – position weld nugget

A comparison of the shape of the welded joint for the material HCT600X + ZF can be observed in Figure 11. From metallographic observations, it can be determined that a dendritic structure was formed in the core of the weld nugget. It can also be deduced that during the joining of the materials, a fusion weld was formed with the characteristic areas of the base material, the heat-affected zone, and the weld nugget. With increasing values of the welding current, hot cracks also occurred in the heat-affected zone. The lack of fusion caused by the shrinkage of weld metal can be seen in the area of the weld nugget. Despite the increasing welding current, the size of the welding nugget did not change rapidly compared to the HCT600X + Z samples.

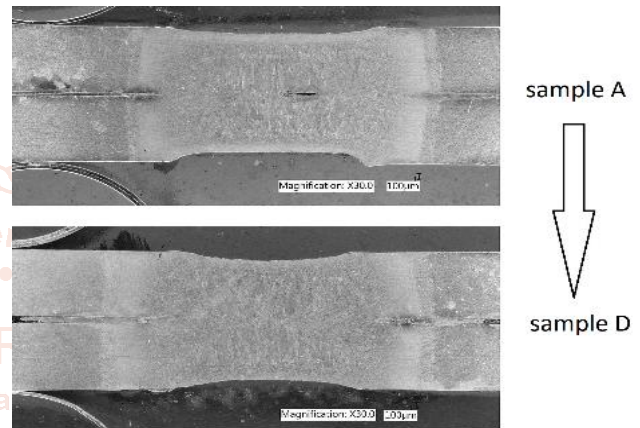


Fig 11 Microstructure of a sample made of HCT600X+ZF

In Figure 12 a transition from the heat-affected zone of the weld to the base material can be observed.

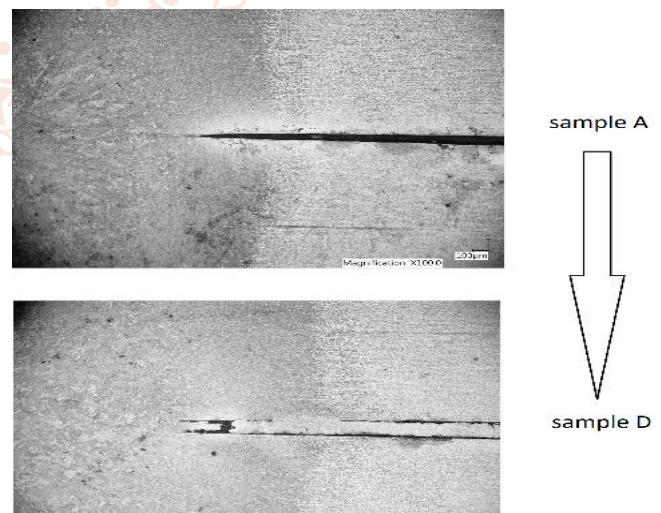


Fig 12 Microstructure of a sample made of HCT600X+ZF – position base material – heat-affected zone

Figure 13 shows the structure of the core in a welded joint.

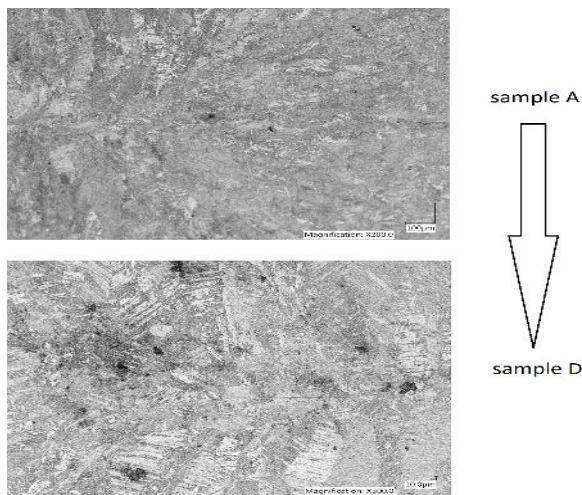


Fig 13 Microstructure of a sample made of HCT600X+ZF – position weld nugget

Conclusion

The paper deals with the evaluation of the join ability of the HCT600X+Z and HCT600X+ZF high-strength steel sheets, where the method - resistance spot welding was investigated. Based on the results of the performed experiments, it can be stated:

- based on the results of the performed experiments, it can be stated that the joints created by resistance spot welding at lower values of welding current were without significant internal defects,
- increasing the welding current led to an improvement in the load-bearing capacity of the joints, but defects such as formation hot cracks were observed,
- this defect is unacceptable in terms of evaluating the quality of joints made by resistance spot welding technology.
- the lowest value of load-bearing capacity of joints was measured on samples with the highest values of welding current (sample A): about 14 kN on the samples with HCT600X+Z, about 12 kN on the samples with HCT600X+ZF,
- the highest value of load-bearing capacity of joints was measured on samples with the highest values of welding current (sample D): about 19.5 kN on the samples with HCT600X+Z, about 17 kN on the samples with HCT600X+ZF.

Acknowledgment

The authors are grateful for the support of experimental works by the project APVV-17-0381 - Increasing the efficiency of forming and joining parts of hybrid car bodies.

References

- [1] Ľ. Kaščák, et al., “Application of modern joining methods in car production,” Processes Examples Strength, Rzeszów, pp.143.
- [2] Vita, et al., “Comparative life cycle assessment of low-pressure RTM, compression RTM and high-pressure RTM manufacturing processes to produce CFRP car hoods,” Procedia CIRP, vol. 80, pp- 352-357, 2019.
- [3] D. Cmorej, et al., “Analýza spájania mikrolegovanej ocele HX420LAD,” Transfer inovácií, vol. 41, pp. 033-038, 2020.
- [4] S. Qin, et al., “Influence of phase and interface properties on the stress state dependent fracture initiation behavior in DP steels through computational modeling,” Materials Science and Engineering: A, vol. 776, 138981, 2020.
- [5] P. R. Spena, “Hybrid laser arc welding of dissimilar TWIP and DP high strength steel weld,” Journal of Manufacturing Processes, vol. 39, pp. 233-240, 2019.
- [6] K. Bzowski, et al., “Application of statistical representation of the microstructure to modeling of phase transformations in DP steels by solution of the diffusion equation,” Procedia Manufacturing, vol. 15, pp. 1847-1855, 2018.
- [7] Ľ. Kaščák, “Vplyv parametrov bodového odporového zvarovania na vlastnosti zvarových spojov,” Košice, Technical university of Košice, pp. 34, 2013, ISBN 978-80-553-1544-7.
- [8] S. Aslanlar, “The effect of nucleus size on mechanical properties in electrical resistance spot welding of sheets used in automotive industry,” Materials & Design, vol. 27, pp. 125-131, 2006.
- [9] L. Plíva, “Odporové svarování v praxi,” SNTL, pp.131, 1963, ISBN 04-219-75.